



Supplement of

Revisited heat budget and probability distributions of turbulent heat fluxes in the Mediterranean Sea

Mahmud Hasan Ghani et al.

Correspondence to: Mahmud Hasan Ghani (mahmudhasan.ghani2@unibo.it)

The copyright of individual parts of the supplement might differ from the article licence.

TABLE OF CONTENTS

Figure S1: Monthly time series of surface averaged heat fluxes for the observed period 2006-2020. The mean value with the solid dashed line is also indicated for each flux component

Figure S2: Monthly time series of surface averaged net heat flux Q_{net} for the observed period 2006-2020. The mean value is indicated with the black dashed line.

Figure S3: Time series of the basin averaged SH, LH, LW and SW overlapped with long-term yearly climatology. Lower quantile boundary lines are marked with dashed lines with different k values used to remove the extremes from the time series.

Figure S4: Comparison of the statistical moments (variance, skewness, kurtosis) computed from the SH flux anomaly series and estimated statistical moments computed using the ALD PDF parameter values

Figure S5: Comparison of the statistical moments (variance, skewness, kurtosis) for observed LH flux anomaly series and estimated statistical moments computed using skew-normal PDF parameter values

Figure S6: Chi-square test statistics computed for the applied PDFs and observed anomalies; ALD PDF for SH flux (left) and Skew-normal PDF for LH flux (right)

Figure S7: Mean annual heat flux components for the period of 2006-2020 computed from ERA5 fluxes (left) and ERA5 inputs (right) using equations (2-10)

Figure S8: Difference map of the ERA5 radiative fluxes (SW+LW) time mean and computed radiative fluxes using ERA5 atmospheric inputs only

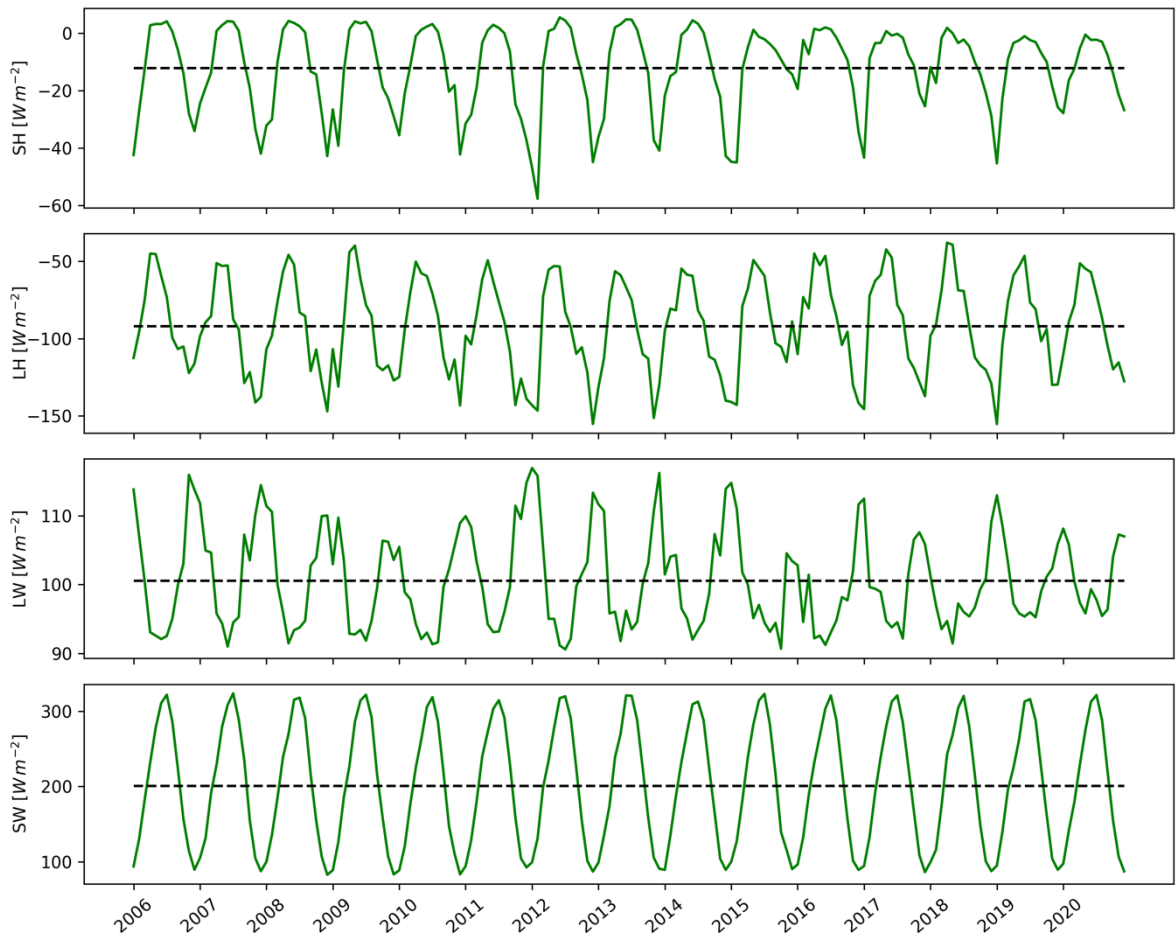


Figure S1: Monthly time series of surface averaged heat fluxes for ECMWF and the observed period 2006-2020. The mean value with the solid dashed line is also indicated for each flux component.

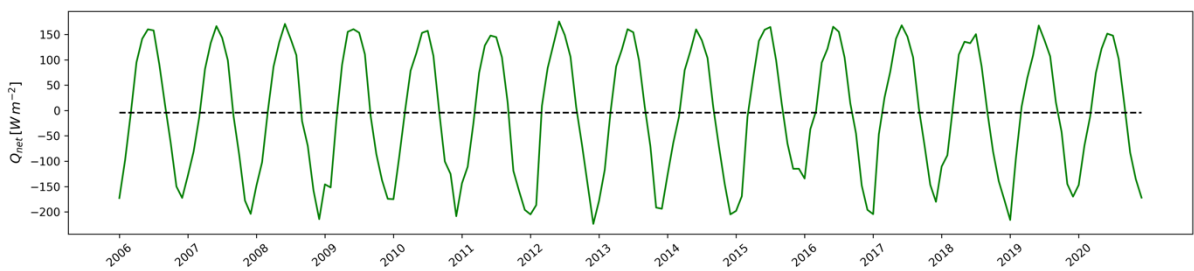


Figure S2: Monthly time series of surface averaged net heat flux Q_{net} for the observed period 2006-2020. The mean value is marked with dashed line

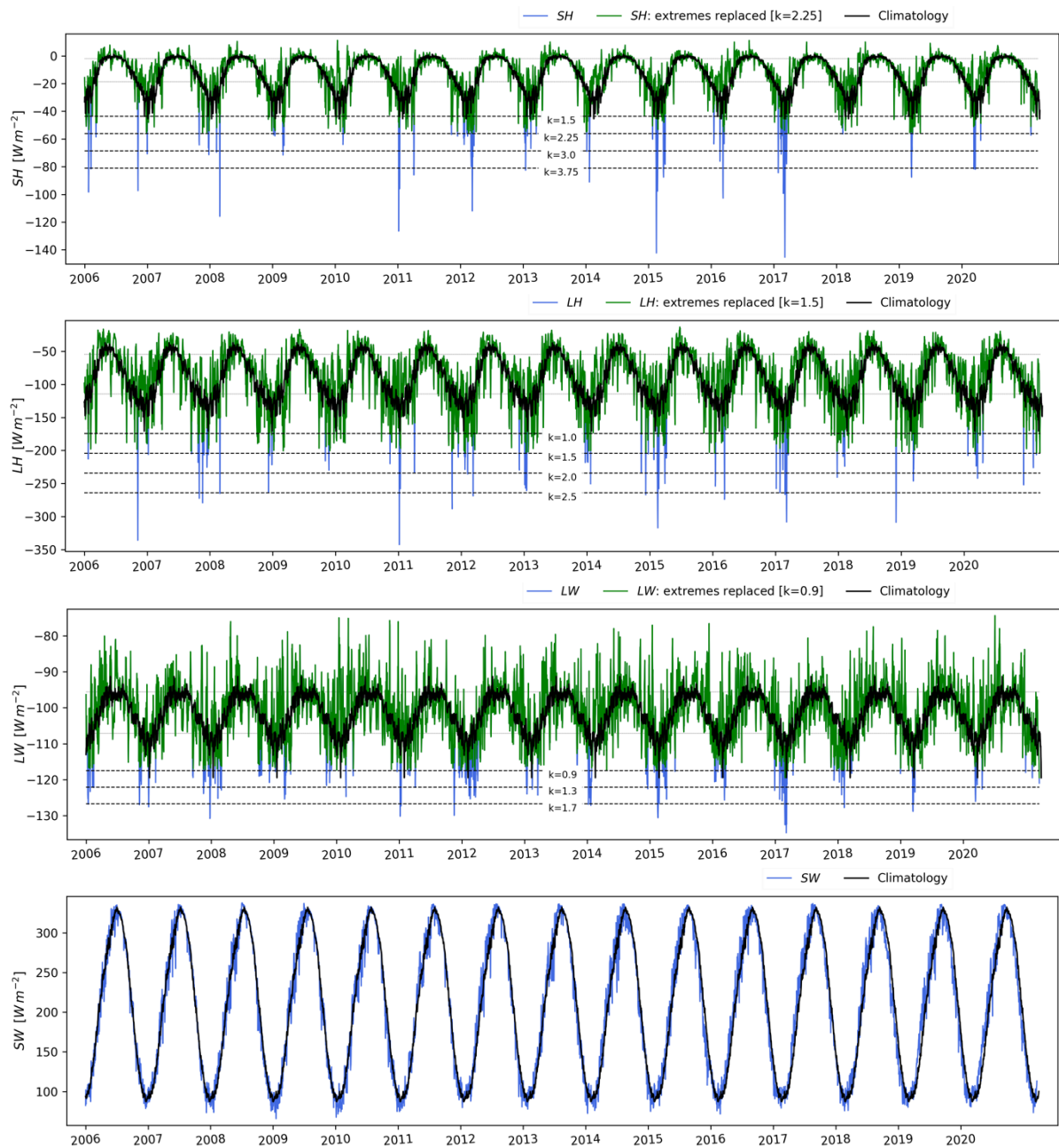


Figure S3: Time series of the basin averaged SH, LH, LW and SW overlapped with long-term yearly climatology. Lower quantile boundary lines are marked with dashed lines with different k values used to remove the extremes from the time series.

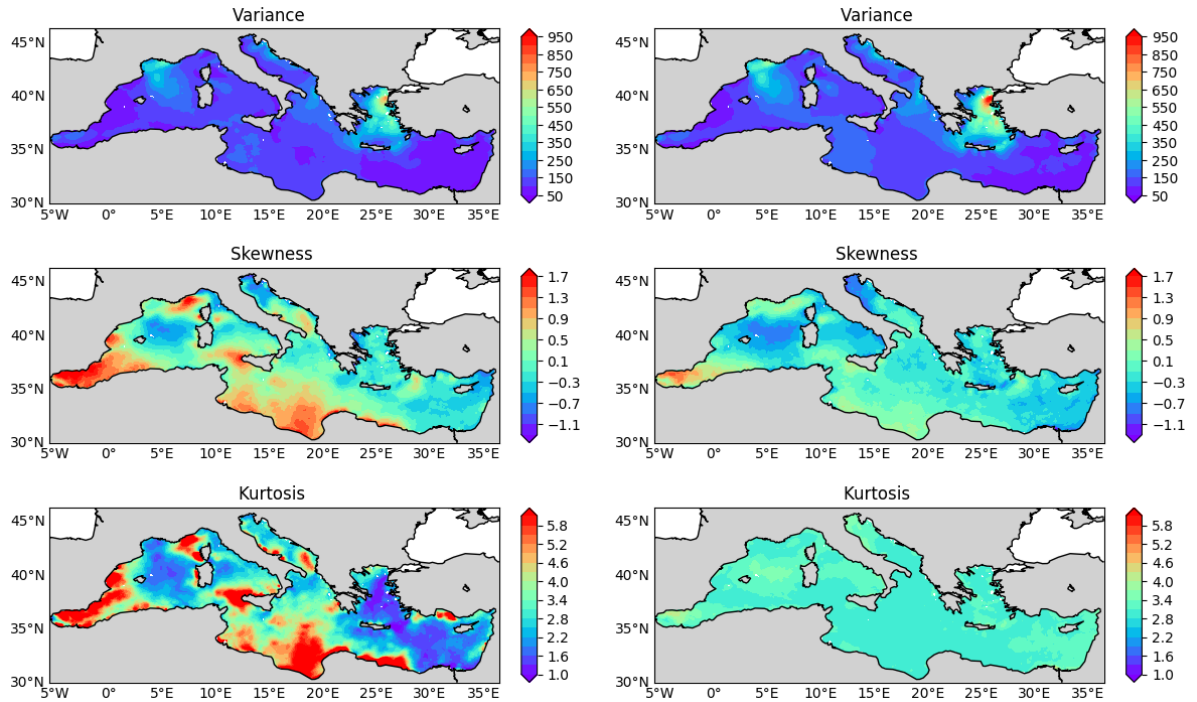


Figure S4: Comparison of the statistical moments (variance, skewness, kurtosis) computed from the SH flux anomaly series and estimated statistical moments computed using the ALD PDF parameter values

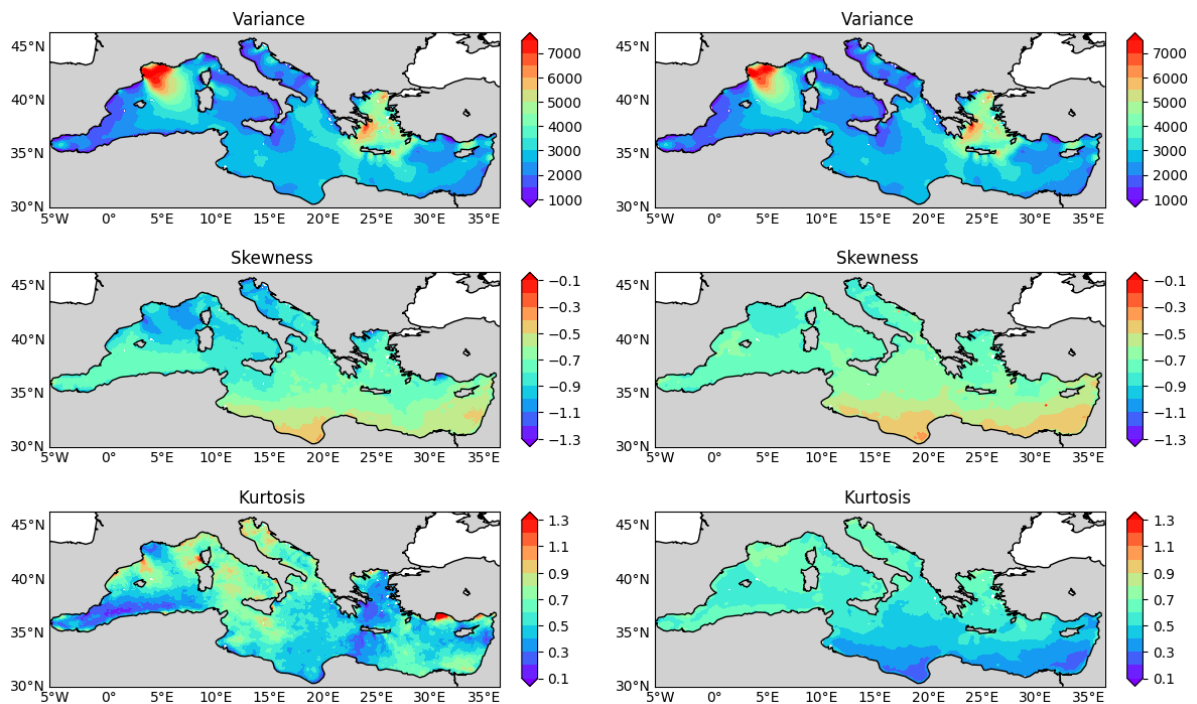


Figure S5: Comparison of the statistical moments (variance, skewness, kurtosis) for observed LH flux anomaly series and estimated statistical moments computed using Skew-normal PDF parameter values

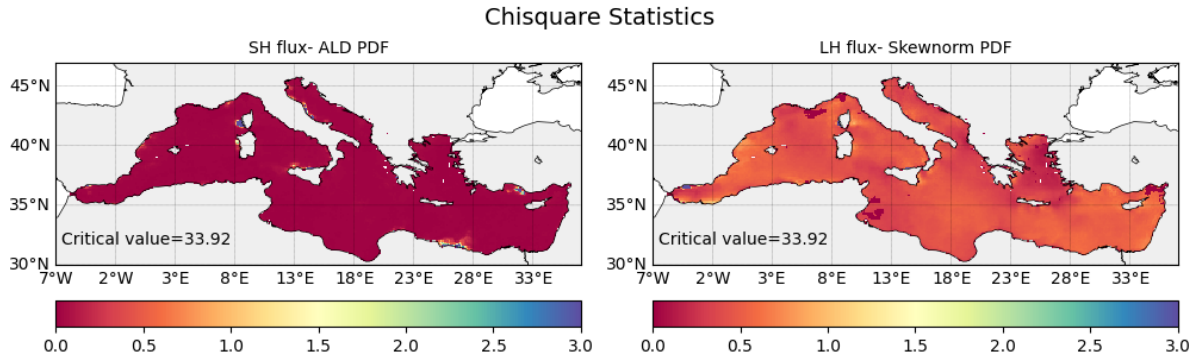


Figure S6: Chi-square test statistics computed for the applied PDFs and observed anomalies; ALD PDF for SH flux (left) and Skew-normal PDF for LH flux (right). All sea grid points values below the critical value (33.92) are theoretically accepted and aligned with applied PDFs.

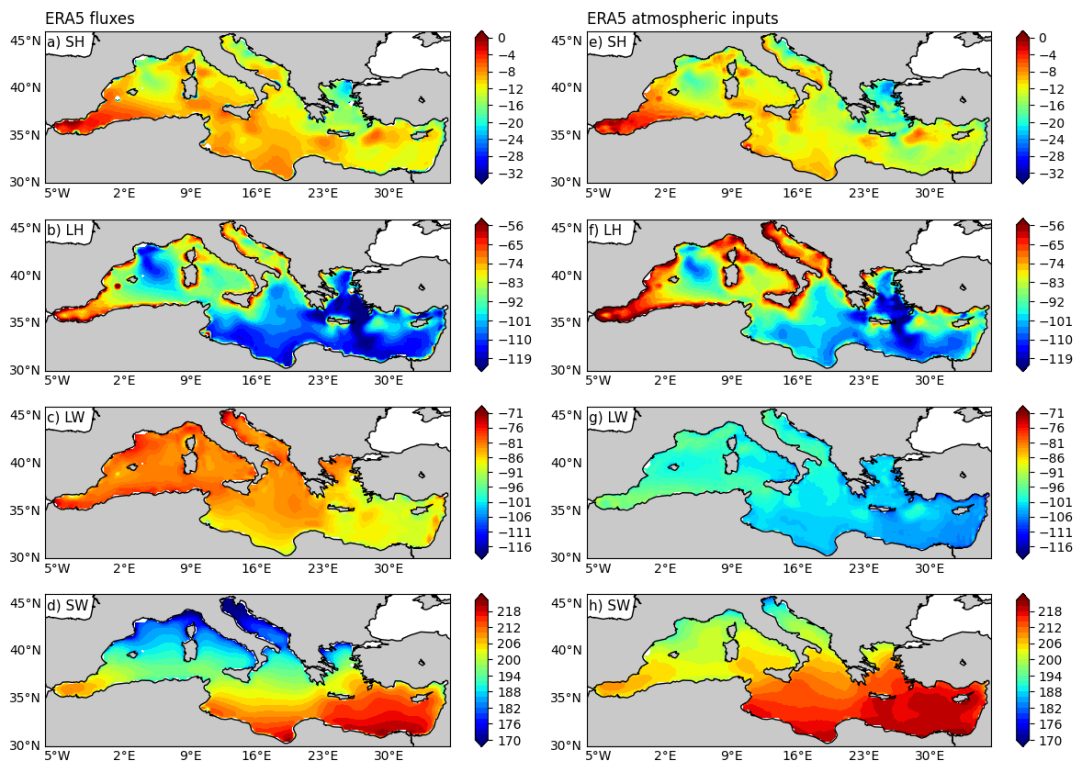


Figure S7: Mean annual heat flux components for the period of 2006-2020 computed from ERA5 fluxes (left) and ERA5 inputs (right) using equations (2-10)

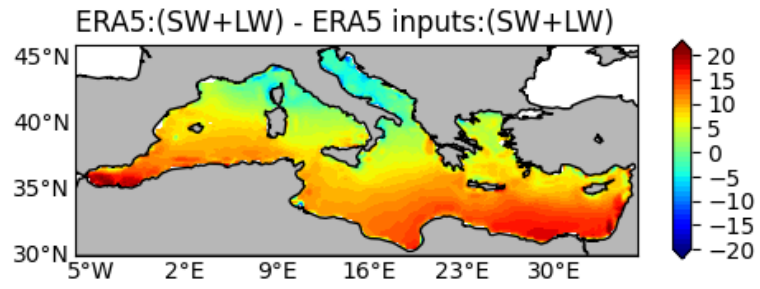


Figure S8: Difference map of the ERA5 radiative fluxes (SW+LW) time mean and computed radiative fluxes using ERA5 atmospheric inputs only.